This is an open access article published under a Creative Commons Attribution (CC-BY) License, which permits unrestricted use, distribution and reproduction in any medium, provided the author and source are cited.

Article

pubs.acs.org/Biomac

"Grafting to" of RAFTed Responsive Polymers to Glass Substrates by Thiol–Ene and Critical Comparison to Thiol–Gold Coupling

Caroline I. Biggs,[†,‡] Marc Walker,[§] and Matthew I. Gibson*[,†,‡]

[†]Department of Chemistry, [‡]Warwick Medical School, and [§]Department of Physics, University of Warwick, Gibbet Hill Road, Coventry, CV4 7AL, United Kingdom

Supporting Information

ABSTRACT: Surface-grafted polymers have been widely applied to modulate biological interfaces and introduce additional functionality. Polymers derived from reversible addition–fragmentation transfer (RAFT) polymerization have a masked thiol at the ω-chain end providing an anchor point for conjugation and in particular displays high affinity for gold surfaces (both flat and particulate). In this work, we report the direct grafting of RAFTed polymers by a "thiol–ene click" (Michael addition) onto glass substrates rather than gold, which provides a more versatile surface for subsequent array-based applications but retains the simplicity. The immobilization of two thermoresponsive polymers are studied here, poly[oligo(ethylene glycol) methyl ether methacrylate] (pOEGMA) and poly(*N*-isopropylacrylamide) (pNIPAM). Using a range of surface analysis techniques the grafting efficiency was compared to thiol–gold and was quantitatively compared to the gold alternative using quartz crystal microbalance. It is shown that this method gives easy access to grafted polymer surfaces with pNIPAM resulting in significantly increased surface coverage compared to pOEGMA. The nonfouling (protein resistance) character of these surfaces is also demonstrated.

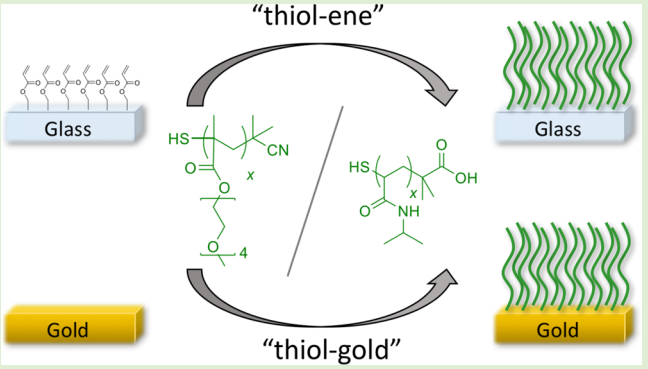

INTRODUCTION

The assembly/immobilization of polymers onto solid supports is technologically useful due to the large variety of their applications, including corrosion, wetting, adhesion, and lubrication control and the associated properties of an ultrathin (<500 nm) grafted layer. It is known that the type of polymer and additionally the grafting density and brush thickness can alter the applications of the surface.[1] Polymers capable of responding to an external stimulus can be incorporated into surfaces to enable switchable behavior[2] and there is particular interest in the biological applications of these systems.[3] Coatings of thermoresponsive poly(*N*-isopropylacrylamide) (pNIPAM) are the classic example and have been widely used as surface coatings to thermally control the detachment of adsorbed cells on 2D cell growth scaffolds.[4] In addition to the pNIPAM coatings, materials functionalized with surface-grafted poly[oligo(ethylene glycol) methyl ether methacrylate] (pOEGMA) have been of great interest to the polymer and materials science community due to their thermoresponsive behavior,[5−8] biocompatibility,[7,8] and resistance to protein and cell absorption.[9] There are two conceptual methods to obtain surface-grafted polymers: (i) "grafting from", where a surface-immobilized initiator is employed, providing a high density polymer brushes; and (ii) "grafting to", where a preformed polymer is covalently attached to a surface. Although "grafting from" gives higher densities and thicker coatings, characterization of the chains is challenging. Conversely, "grafting to" is limited in the density and thickness that can be achieved but is conceptually simpler and enables full characterization of the polymer, which is useful to eliminate batch-to-batch variability. To enable "grafting to" a reactive end-group is required that can undergo an efficient and preferably orthogonal coupling reaction. Various functional groups have been employed for this, such as active esters, azide/alkyne "click" and thiol–ene Michael addition processes.[10,11] Plasma polymerization can also be used to generate highly branched and highly cross-linked polymers. This produces highly dense and controllable layers and removes the need for grafting but is limited by the requirement for ionizable monomer species.[12] Hydrogels can also offer a route to biologically interesting polymer coatings. For example, poly(*N*-alkyl acrylamide) and poly(urethane) hydrogel coated glass has been investigated for its resistance to platelet adhesion[13] and physically cross-linked nanogels of branched poly(ethylene imine) have been used to form antimicrobial ultrathin films on mica and graphite.[14]

One of the most convenient methods for formation of grafted layers is thiol–gold immobilization (e.g., self-assembled monolayers) and has been widely applied.[15] Inspired by this, McCormick et al. utilized polymers synthesized by RAFT (reversible addition–fragmentation transfer) polymerization for immobilization onto gold surfaces.[16] RAFT not only gives control over molecular weight, dispersity, and is tolerant to most functional groups but

Received: May 10, 2016
Revised: July 7, 2016
Published: July 13, 2016

 © 2016 American Chemical Society

DOI: 10.1021/acs.biomac.6b00662
Biomacromolecules 2016, 17, 2626−2633

also installs a protected thiol (via dithioester, trithiocarbamate, or xanthate typically) at every chain end, making it ideal for gold-grafting. For example, Gibson et al. have produce gold nanoparticle libraries based on RAFT[17] or glycopolymer coated gold particles.[18] While a useful method, gold substrates are neither cheap nor applicable to a range of analytical techniques (with the obvious exception of surface plasmon resonance). Conversely, the use of glass substrates for (micro)array applications has revolutionized our understanding of many biochemical processes by enabling high throughput analysis using minute quantities of ligands.[19] A key characteristic required for successful arrays is the presentation of the ligand at the interface. However, a nonfouling surface, which prevents unwanted protein/cell interactions, is also desired in order to reduce false positive results on the arrays. The addition of hydrophilic polymer such as PEG improves this,[20] but PEG is limited in terms of the chemical space for attachment chemistry and is synthesized by anionic polymerization, which is more challenging than controlled radical polymerization.

Considering the above, here we report the study of the "grafting to" of RAFTed polymers onto glass slides, which have been modified to enable a thiol−ene "click" reaction, to combine the benefits of thiol−gold with the utility of a glass slide. The interaction is studied in detail by a range of analytical techniques and the potential as a substrate for a microarrays analysis system is demonstrated.

EXPERIMENTAL SECTION

Materials and Methods. All reagents and solvents were used as received from the supplier. Laboratory solvents were purchased from Fisher Scientific, 3-(trimethoxysilyl)propyl acrylate from Sigma-Aldrich. Microscope slides were purchased from Fisher Scientific (ground edges, plain glass, product code: 12383118) and silicon wafers from IDB Technologies with a resistivity of 1−10Ω. Ten millimoles HEPES buffer, containing 0.1 mmol $CaCl_2$, pH 6.5, was prepared in 250 mL of Milli-Q water. Ethanolamine and monomers were purchased from Sigma-Aldrich and fluorescently labeled lectins (PNA, ConA) from Vector Laboratories (Fluorescein FLK-2100 labeled).

Contact Angle Measurements. The water contact angle measurements were conducted at room temperature using a Krüss drop shape analysis system DSA100 equipped with a movable sample table and microliter syringe. Full experimental details are included in the Supporting Information.

Ellipsometry. Ellipsometry measurements were carried out on a Nanofilm autonulling imaging ellipsometer with a resolution of 0.001° (delta and psi). A 550 nm wavelength light source was used and all measurements were taken using an angle of incidence scan at 50, 60, and 70° using four zone nulling. Full experimental details are included in the Supporting Information.

X-ray Photoelectron Spectroscopy. The samples were mounted on to a sample bar using electrically conductive carbon tape and loaded in to the fast-entry chamber of the Kratos Axis Ultra DLD spectrometer. Once the fast-entry chamber had been evacuated to an appropriate pressure, the samples were transferred in to the analysis chamber for data acquisition at pressures of less than 1×10^{-9} mbar. Core level XPS spectra were recorded using a pass energy of 20 eV (approximately 0.45 eV resolution) with the sample illuminated using an Al K α X-ray source ($h\nu$ = 1486.6 eV). Analysis of the XPS data was carried out using the Casa XPS software using mixed Gaussian−Lorentzian (Voigt) lineshapes. The transmission function of the analyzer has been carefully determined using clean Au, Ag, and Cu foils, while the work function of the analyzer was determined using the Fermi edge of a polycrystalline Ag sample at regular intervals throughout the experiment, thereby allowing accurate composition and binding energy shifts to be determined. All binding energies have been referenced to the C 1s peak arising from adventitious carbon at 284.6 eV, a necessary correction due to the insulating nature of the insulating nature of the oxide termination of the Si substrate.

Microarray Scanner. The fluorescence images were obtained using an Agilent G2565CA Scanner with a 2 μm resolution. Standard two color scanning protocols were used with a SHG-YAG laser (532 nm) and a helium−neon laser (633 nm). The samples were loaded and the standard two color scan was run, producing the data as a tagged image file (TIF). The resulting image files were analyzed using Agilent Feature Extraction Software. The average fluorescent intensity was calculated for the sample area of interest by taking the average output value for the green channel for that set area. The background fluorescence (the average output value for the green channel for all of the areas of the sample without a lectin spot) was calculated manually and subtracted.

Quartz-Crystal Microbalance with Dissipation. Gold and silicon QCM sensors were purchased from Q-Sense. The sensors have a resonant frequency of 4.95 MHz ± 50 kHz with a diameter of 14 mm and a surface roughness of ≤3 nm. The experiments were carried out using a Q-Sense E4 QCM-D instrument with the temperature set to 30 °C throughout the experiments, using the in-built temperature controller. The surfaces were cleaned with piranha solution prior to use. Should a sensor have been stored between cleaning and testing, it was rinsed (ethanol 2 × 5 mL and water 2 × 5 mL) and dried with nitrogen, immediately prior to usage. Solutions of pOEGMA and pNIPAM (2 mg mL^{-1} in water with and without amine) were prepared and sonicated and thermally equilibrated for 20 min prior to the experiment in order to remove any air from the solutions. The sensors were placed in the chambers and sonicated Milli-Q water was pumped at a rate of 200 $\mu L \cdot min^{-1}$ until the sensors' resonant frequencies equilibrated. The bathing solution was then changed to 2 $mg \cdot mL^{-1}$ of the relevant polymer and allowed to equilibrate, whereupon the solution was changed back to water to remove any polymer simply resting on the surface and the flow was continued until a stable baseline was achieved. At each solution change, the pump was stopped and restarted to avoid any air intake to the system. Following the experiment, the system was cleaned (sodium dodecyl sulfate, 2 $mg \cdot mL^{-1}$, followed by water, both pumped over at maximum speed for 10 min each) in order to remove any remaining traces of unbound polymer. The sensors were washed with water and dried with nitrogen and then stored in their original boxes until they were cleaned for use in a further experiment.

The silicon sensors were placed into the QCM-D machine either in their native state (chemically cleaned silicon surface) or having been

Table 1. Polymer Characterisation Data

polymer[a]	[M]/[CTA]	conversion[b] (%)	$M_{n,Theo}$[c] (g mol^{-1})	$M_{n,SEC}$[d] (g mol^{-1})	M_w/M_n[d]	CP[e] (°C)
$pOEGMA_{25}$	25:1	80	3100	5000	1.24	82.9
$pOEGMA_{50}$	50:1	85	6300	7200	1.28	78.2
$pOEGMA_{100}$	100:1	85	12000	11000	1.33	75.4
$pNIPAM_{25}$	25:1	95	2700	1500	1.21	60.2
$pNIPAM_{50}$	50:1	95	4200	6200	1.23	53.6
$pNIPAM_{100}$	100:1	95	11000	8600	1.23	46.2

[a]NIPAM = *N*-isopropylacrylamide; OEGMA = oligo(ethylene glycol) methyl ether methacrylate. [b]Conversion determined by ^{1}H NMR spectroscopy. [c]Determined by ^{1}H NMR spectroscopy relative to an internal standard (mesitylene). [d]Determined by SEC (DMF) relative to PMMA standards. [e]CP = Cloud point at polymer concentration of 1 $mg \cdot mL^{-1}$ in PBS.

DOI: 10.1021/acs.biomac.6b00662
Biomacromolecules 2016, 17, 2626−2633

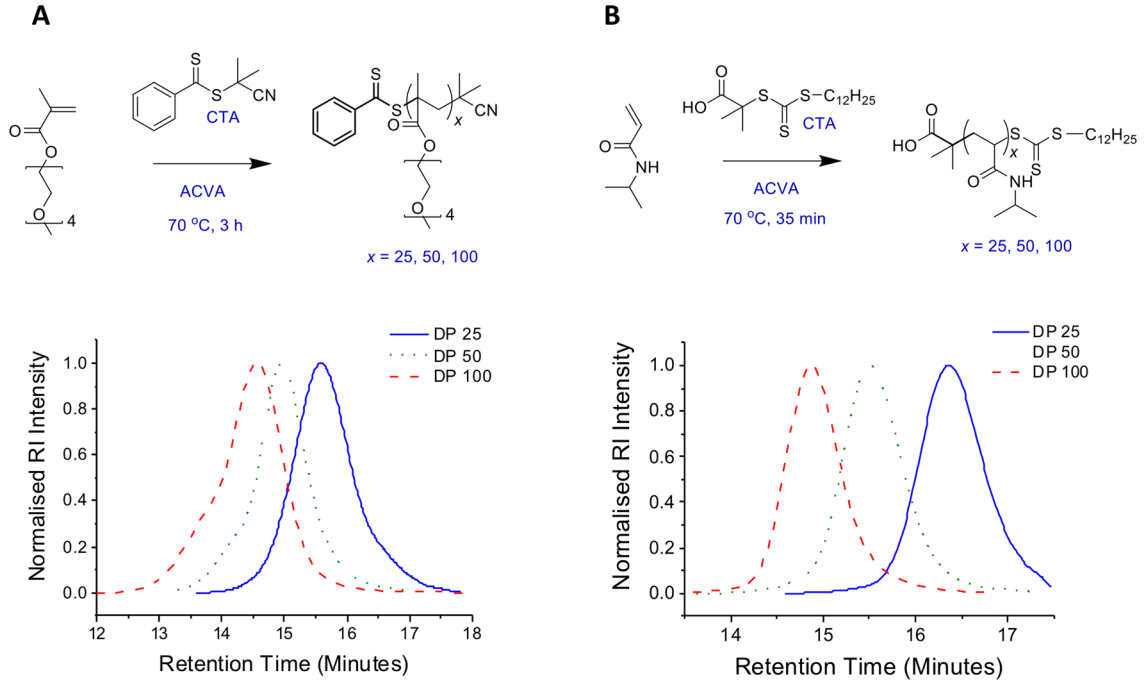

Figure 1. Polymers synthesized in this work and corresponding SEC traces. (A) pOEGMA and (B) pNIPAM.

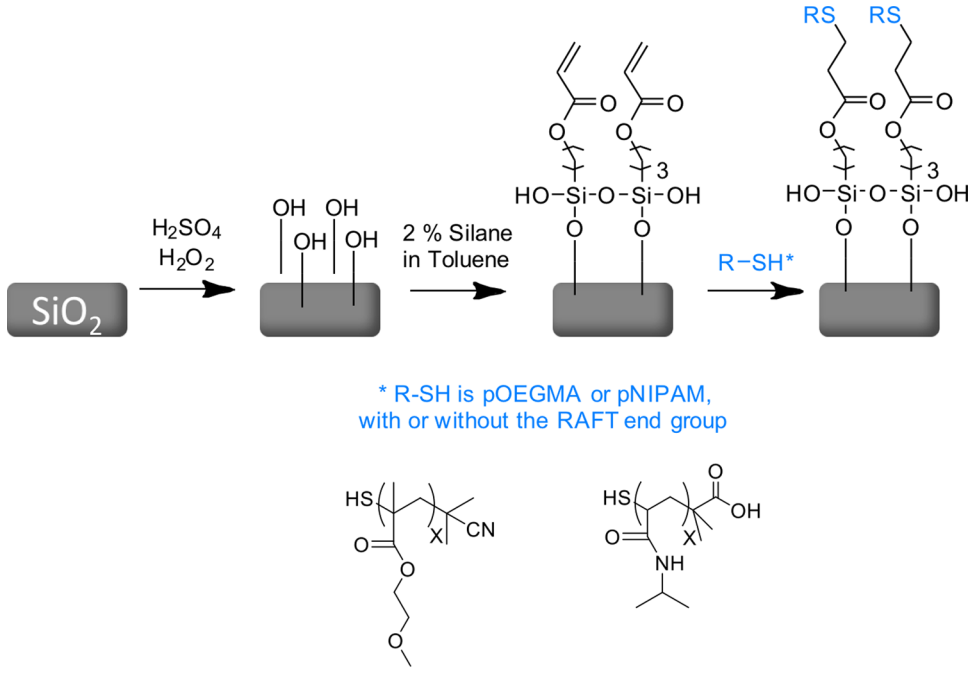

Figure 2. Schematic representation of the immobilization of polymers onto acrylate silane functionalized glass and silicon surfaces.

previously functionalized with silane. The experiments were then carried out as for the gold sensors.

Experimental Procedures. *Surface Cleaning.* The solid surfaces used in this work (glass slides and silicon wafers) were cleaned using piranha solution [caution: reacts violently with organic material]. The surfaces were placed into a 3:1 (v/v) mixture of 98% sulfuric acid and 30% hydrogen peroxide, on ice, for 20 min, then rinsed with deionized water and dried in a gentle stream of dry nitrogen.

Silanization and Control Surfaces. Immediately following the cleaning process, the samples were immersed into a solution of 3-(trimethyoxysilyl)-propyl acrylate (5 mL, 2% v/v in toluene, 2 h, RT), washed with toluene (5 × 2 mL) and water (5 × 2 mL), then blown under a stream of nitrogen until dry. This process applied to the glass slides and the silicon wafers.

Polymer Functionalization of Silane-Coated Surfaces. Following silanization, the samples were immersed into the chosen polymer solution (2 mg·mL^{-1} in water) for 2 h (RT), then washed with distilled water (3 × 2 mL), and dried under a stream of nitrogen. For the samples that were functionalized in the presence of amine, ethanolamine (0.1 mL) was added into the polymer solution prior to addition of the sample.

Lectin Binding Studies. Samples were subjected to spots (20 μL) of the relevant fluorescently labeled lectins (0.1 mg.mL^{-1} in HEPES) for 30 min (RT, dark). The protein solutions were then removed by pipet and the surface was washed (2 × 5 mL appropriate buffer, 5 × 5 mL deionized water) and dried under a stream of nitrogen.

DOI: 10.1021/acs.biomac.6b00662
Biomacromolecules 2016, 17, 2626−2633

RESULTS AND DISCUSSION

The polymers in this study were synthesized using RAFT polymerization as it ensures the (quantitative) installation of a thiol-group at each chain end for subsequent (bio-orthogonal) surface immobilization (vide infra). As "grafting to" immobilization of polymers onto surfaces is limited by the steric hindrance of the polymer chains, only relatively short chains were employed, justifying the use of RAFT, which provides good control in the size range of interest. $pOEGMA_{300}$ and pNIPAM were polymerized using 2-cyano-2-propyl benzodithioate (CPBD) and 2-(dodecylthiocarbonothioylthio)-2-methylpropanoic acid, respectively (see Supporting Information for synthetic details) as representative responsive polymers. Monomer-to-CTA ratios of 25, 50, and 100 were used to generate a focused library of differing molecular weights; see Table 1. The resulting polymers were characterized by ^{1}H NMR spectroscopy and size-exclusion chromatography (SEC) indicating good control over molecular weight and dispersity (Figure 1 and Table 1). The SEC values for M_n agreed well for the shorter polymers, but for longer ones there was more deviation due to an underestimation of the molecular weight arising their brush-like structure in solution, as is commonly seen for these polymers.[21] From this point, the DP estimated by [M]/[CTA] will be used as the quoted value for discussion. Both sets of polymers synthesized in this work are expected to show LCST behavior in aqueous solution. This was evaluated by turbidimetric analysis (actual curves in the Supporting Information) and the observed cloud point (macroscopic effect associated with LCST) reported in Table 1. For both polymer types, as the chain length is increased the cloud point decreases, as would be expected. The pNIPAMs exhibit cloud points that are higher than might be expected due to a combination of their relatively short length and carboxylic acid end group, both of which increase the transition to above the often cited value of 32 °C.[21,22]

With this library of polymers to hand, they could be evaluated for "grafting to" surfaces with the longer term aim of them being suitable for (micro)arrays. Array applications require glass slides as the solid substrates to allow for subsequent analysis by automated scanning fluorescence binding assays, but the majority of "grafting to" applications for RAFT involve immobilization onto gold (c.f self-assembled monolayers).[23] We have previously demonstrated that thio-glycosides could be immobilized onto acrylate-functionalized glass surfaces via thiol−ene "click" (i.e., Michael addition)[24] and rationalized that this would also be compatible with RAFT-derived polymers bearing a thiol-end group to enable their direct immobilization onto glass, Figure 2. This can be considered as an analogy to thiol−gold immobilization, which is widely used but limited by the need for the gold substrate restricting the ultimate application.

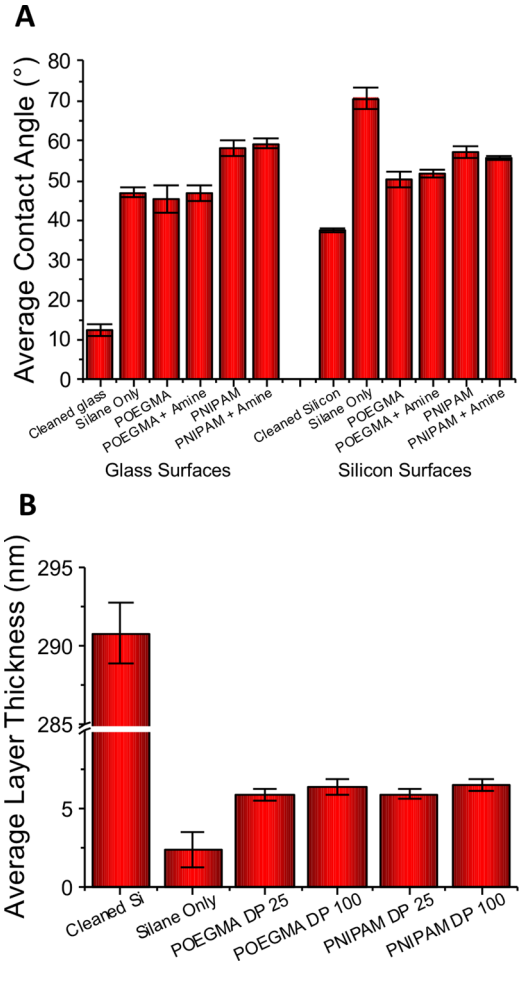

Figure 3. Analysis of surface-grafted polymers. (A) Contact angle analysis. (B) Layer thicknesses determined by ellipsometry on silicon wafers. Indicated thickness is of each individual layer, not cumulative thickness. Error bars represent standard deviation from minimum of three independent measurements.

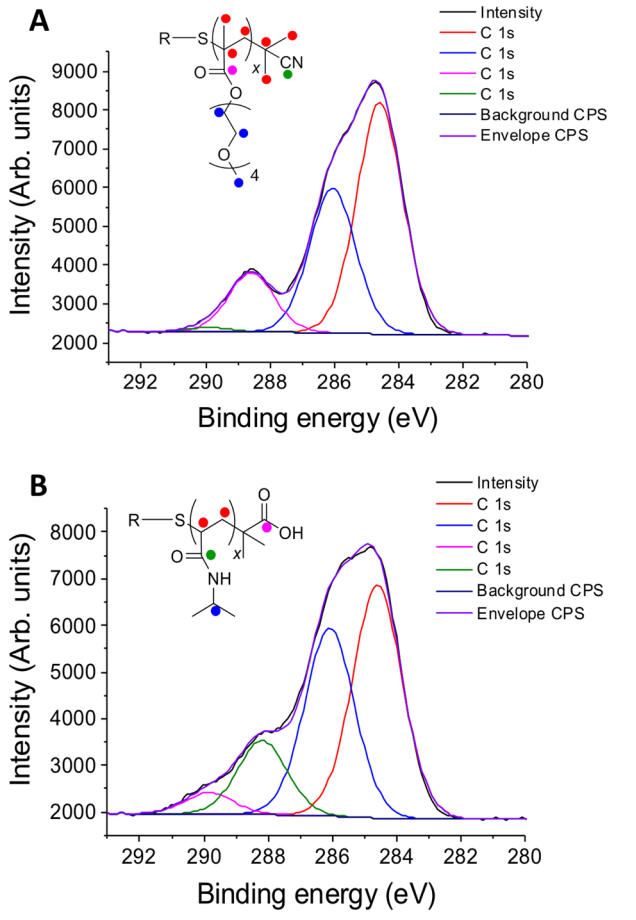

Figure 4. XPS spectroscopy analysis. (A) Representative high-resolution spectrum of the C 1s for pOEGMA coated silicon. (B) Representative high-resolution spectrum of the C 1s for pNIPAM coated silicon. Data is shown for x = 25.

DOI: 10.1021/acs.biomac.6b00662
Biomacromolecules 2016, 17, 2626−2633

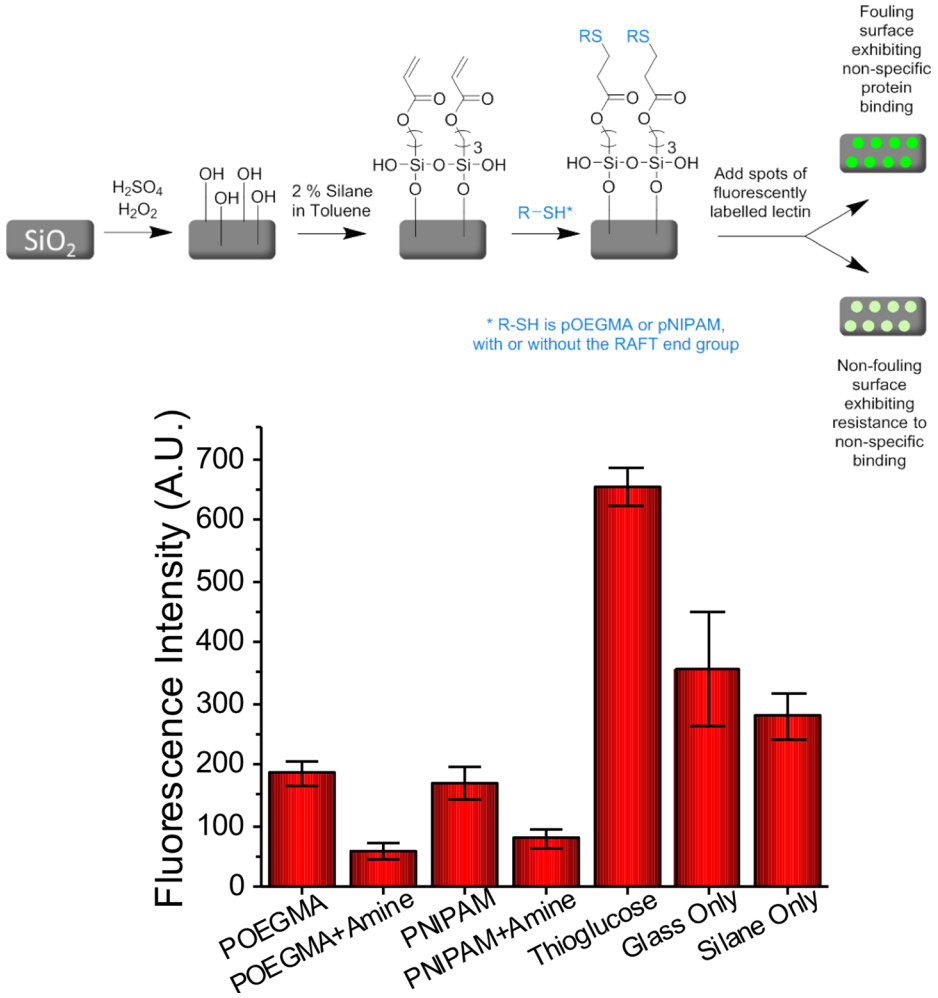

Figure 5. Nonspecific protein adhesion analysis. ConA-FITC was used as the protein with thio-glucose providing a positive control. Error bars represent standard deviation from a minimum of three independent measurements.

To prepare the glass slides, they were first cleaned using "piranha solution" [CAUTION: Extreme care must be taken when handling this; see Experimental Section before attempting] and then functionalized with 3-(trimethoxysilyl)propyl acrylate by solution phase deposition from toluene. In parallel, silicon wafers were also functionalized in the same manner to enable full chemical characterization using XPS (X-ray photoelectron spectroscopy) and ellipsometry, which are both more challenging to conduct on glass, in addition to drop shape analysis (DSA) that works for both surfaces.[25] These surfaces were incubated with polymers that had their RAFT agents cleaved by addition of ethanolamine, as this has the secondary benefit of catalyzing the thiol−ene reaction.[10]

Figure 3 shows the static water contact angle measurements for glass and silicon surfaces with both pOEGMA and pNIPAM coatings. Upon addition of the polymers the contact angles increase from 10° (glass) and 40° (silicon) to around 50° as would be expected for this class of polymer. The role of added amine was not clear from the DSA analysis. While amine is known to catalyze the thiol−ene reaction, DSA is not necessarily sensitive to the amount of material grafted, as we have previously reported using thio-glycosides.[24] The differences in absolute contact angles between glass and silicon is likely due to the complex dependence of contact angle on the roughness of the substrate, especially for static angles.[26] Consistently across the two substrates, the pOEGMA coatings exhibit lower contact angles than pNIPAM coatings, corresponding with the hydrophilic nature of the pOEGMA structure. The thickness of the polymer coatings on the silicon surfaces was investigated using ellipsometry and modeled using a three layer model, Figure 3B. All the polymer coatings gave a thickness of 6−7 nm and the differences between the different polymer types and chain lengths are not significant. Previous work in this area has found that pNIPAM brushes grafted to silicon substrates form brushes with a dry thickness of 3−24 nm, which is comparable with our results.[27] It is important to note that the silicon wafers used in this study contain a very thick oxide layer (~290 nm), which is incorporated into the model, but large compared to the thin polymer coating. However, the results obtained are realistic for partially coiled polymers of these lengths and the ellipsometry measurements (along with the DSA) serve to supplement the QCM-D analysis (vide infra).

XPS was employed to characterize the polymers grafted to silicon wafers and to provide chemical evidence of attachment (additional data in the Supporting Information), Figure 4. The assigned spectra for C 1s peaks in pOEGMA and pNIPAM coatings are shown. In each case the most numerous carbon environment, corresponding to those carbon atoms present on the polymer backbone, indicated in red, results in the highest

DOI: 10.1021/acs.biomac.6b00662
Biomacromolecules 2016, 17, 2626−2633

intensity peak. The intensity of the remaining peaks is also seen to appear in order of their prevalence within the structure.

The conjugation of the polymers to the surface should modify their interfacial properties in particular nonspecific protein adsorption (relevant for array applications). Fluorescently labeled Concanavlin A (ConA) (an α-glucose/mannose binding protein that we have interest in using for glycomics applications)[28] was incubated with the glass surfaces (with and without polymer) for 30 min and subsequently washed and dried, Figure 5. The extent of protein binding was visualized using a fluorescence array scanner. A positive control using glucose-functionalized glass slides was employed (for specific interaction with the ConA). The native glass and silane-coated slides showed significant nonspecific absorption of the protein as would be expected and highlighting the need for protein-resistant coatings. Both pOEGMA and pNIPAM coatings resulted in significant decreases in protein binding due in part to their hydrophilic nature, confirming successful attachment and modulation of the surface properties.[21,29,30]

Quartz-Crystal Microbalance Analysis. This "grafting to" approach is appealing, enabling full polymer characterization prior to surface immobilization, and reducing batch-to-batch variability. However, the attachment of thiol-terminated polymers onto gold substrates remains the current standard despite the price of the substrates and limited application. We therefore employed a quartz-crystal microbalance with dissipation (QCM-D) instrument in order to provide more in-depth analysis of the "grafting to" both gold and acrylate surfaces. This technique enables both the kinetics of the process (i.e., how long is required to achieve maximum coverage) and the total mass absorbed to be studied and to identify subtle differences between the two classes of polymer, which the macroscopic measurements do not reveal. The QCM-D monitors the change in frequency (f) of the underlying quartz crystal with an increase in surface mass represented by a decrease in resonant frequency.[31] At the same time, the dissipation (D) of the system is also recorded, providing information on the rigidity of the films or brushes which are being formed. An absorbed layer with a high ΔD is said to be soft, whereas a low ΔD indicates rigidity.[32]

$POEGMA_{25}$ was flowed over a piranha- [CAUTION: see Experimental Section before using this reagent] cleaned gold sensor at a concentration of 2 $mg{\cdot}mL^{-1}$, which was found to be sufficient in initial screenings, at a flow rate of 200 $\mu L{\cdot}min^{-1}$. Prior to adding the polymer, the sensors were equilibrated under a flow of Milli-Q water for at least 30 min. At the end of the exposure to the polymer solution, any noncovalent bound polymer was removed by flowing over Milli-Q water again, to ensure that only the frequency change associated with the attached polymers was investigated, which avoids false positive results. Additional experimental considerations can be found in the Supporting Information. The QCM-D traces (Figure 6) show that as the polymer is added the frequency decreases, thus indicating increased mass on the surface. The low dissipation changes also confirms that the polymers are producing a rigid film that fully couples to the sensor.[31] As for the pOGEMAs, the pNIPAMs were also applied to the sensor, resulting in frequency shifts indicative of binding, Figure 7A. Comparison of the total Δf for each of the polymers is shown in Figure 7B. Clearly the pNIPAMs resulted in increased mass of polymer being attached to the gold compared to corresponding chain lengths of pOEGMA, with a comparative QCM trace for both polymers with DP = 25 shown in Figure 7C. There was little chain length dependence on Δf for the pOEGMAs, suggesting that in this DP range the limiting factor for grafting was the steric hindrance of the OEG side chains.

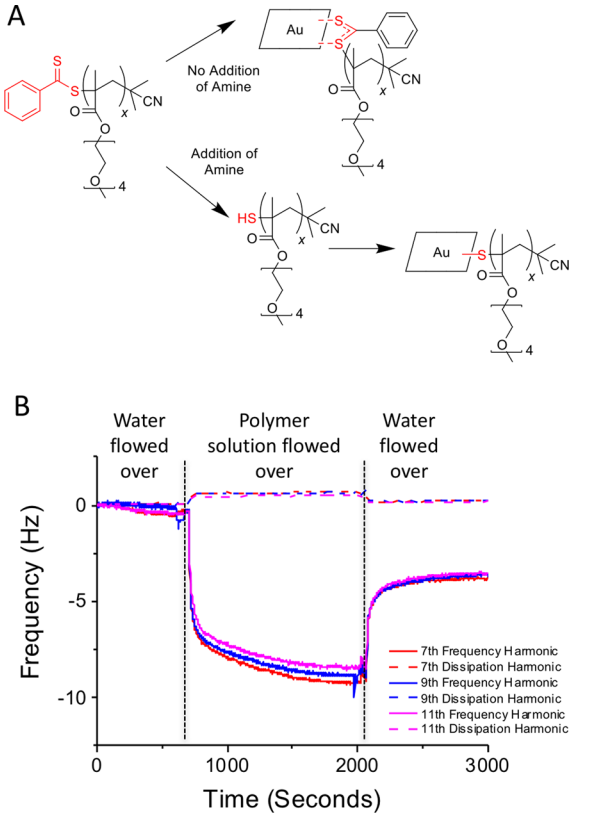

Figure 6. (A) Self-assembly of pOEGMA polymers onto a gold surface via thedithioester RAFT end group (no amine) or free thiol end group (addition of amine). (B) Typical QCM-D trace for the grafting of $pOEGMA_{25}$.

However, for pNIPAM the shorter polymers clearly grafted to higher amounts than the longer ones, suggesting that chain-length is the limited factor.

Analysis of the polymer grafting mass is shown in Figure 7. For pOEGMA samples, all three chain lengths resulted in similar shifts. For adsorbed films with only small ΔD values, the adsorbed mass is proportional to the change in frequency and the Sauerbrey equation may be applied. Figure 7D shows this analysis for DP 25 polymers that would suggest that pNIPAM had around 10-fold increase in grafting density relative to the pOEGMA. It should be noted that the Sauerbrey equation is only an approximation in this regime. A key finding is that the DSA analysis (above) did not reveal these differences in grafting, validating the combined use of multiple analytical techniques. For future applications, the density of chains is crucial, as they would be used for the attachment of biological binding ligands (e.g., sugars) so maximizing the number of chains will ensure the highest possible density of binding ligands.

A comparison was then undertaken between thiol−gold immobilization and thiol−acrylate (i.e., the desired application). For this, the gold QCM-D sensors were replaced with SiO_2-coated QCM-D sensors providing a glass-like surface that could be modified to install the acrylate groups. Figure 8 shows the frequency changes upon flowing pNIPAMs over both the acrylate and the SiO_2 sensors as a negative control. Despite an initial sharp Δf when the polymer is flowed over the SiO_2 surface (see Supporting Information for QCM-D trace), when the solution is reverted to water this change is reversed and the frequency shifts back to the original baseline at 0 Hz. This confirms that no polymer is adsorbing onto the SiO_2, as would be expected, and also emphasizes the importance of recording frequency values postwashing. However, when

DOI: 10.1021/acs.biomac.6b00662
Biomacromolecules 2016, 17, 2626−2633

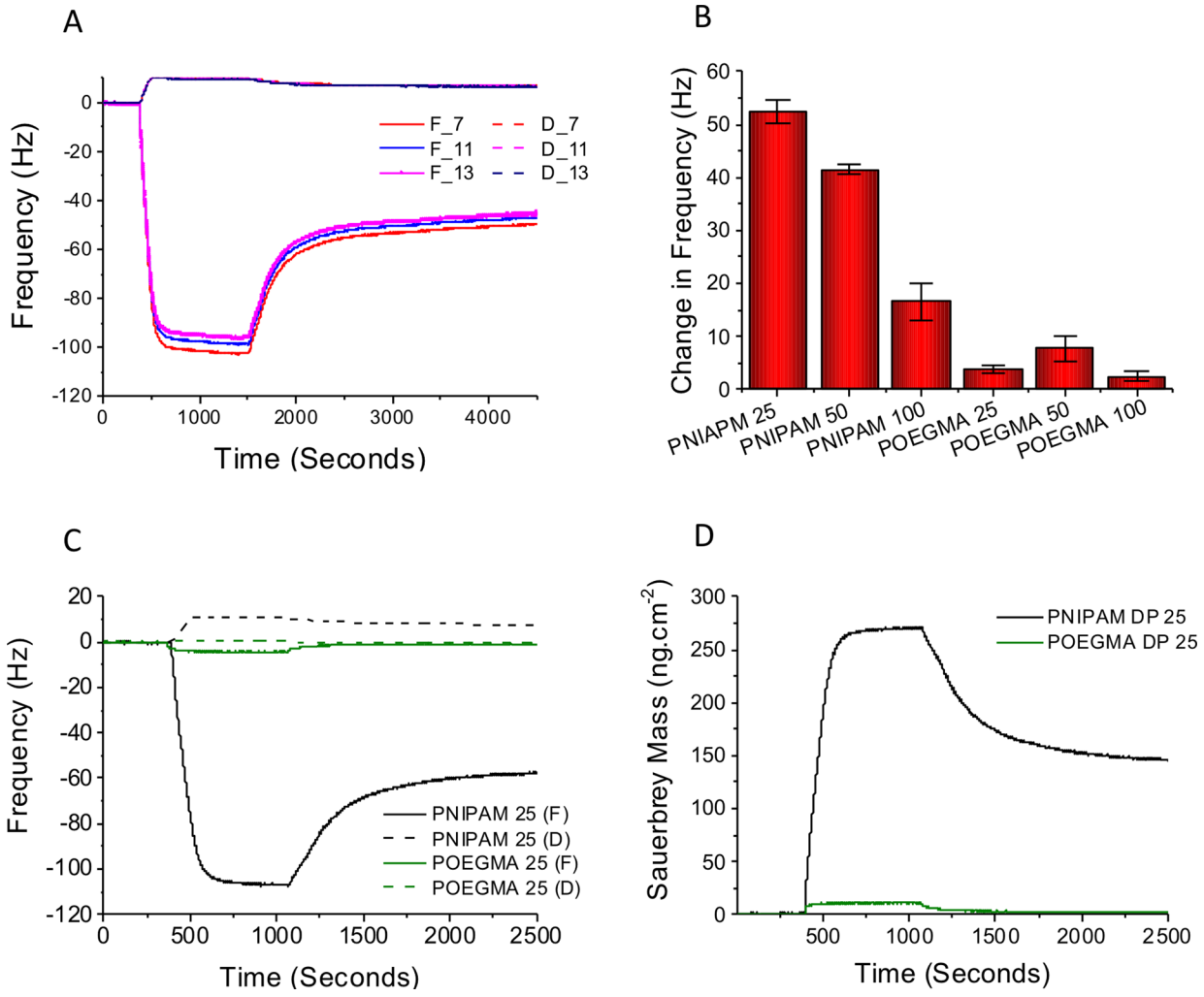

Figure 7. QCM analysis of polymer binding to gold surfaces. (A) QCM trace for $pNIPAM_{25}$. (B) Average change in frequency value attributed to the binding of each polymer. (C) QCM-D traces comparing $pOEGMA_{25}$ and $pNIPAM_{25}$. (D) Sauerbrey mass changes upon binding of $pOEGMA_{25}$ and $pNIPAM_{25}$. Data taken from at least three independent repeats for each sample.

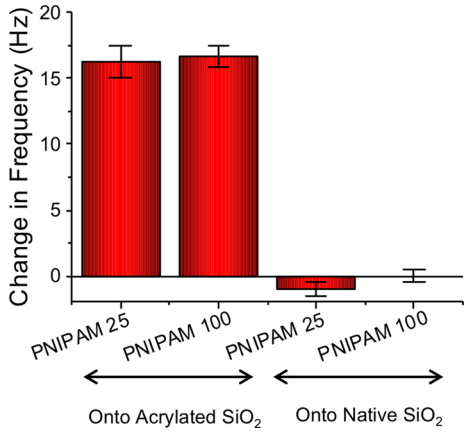

Figure 8. Change in frequency after flowing pNIPAMS over sensors. Errors bars are standard deviation from a minimum of three repeats.

the acrylate surfaces are used, there was a clear shift in frequency even after washing, indicating successful conjugation of the RAFTed polymers onto the surface. The calculated Sauerbrey mass changes associated with this experiment are shown in Figure 9. The absolute frequency shifts seen were less than for gold, which may be due to the density of the acrylate groups. This is supported by the observation that the DP 25 and DP 100 both gave equal grafting masses, which is consistent with acrylate spacing being the limiting factor and not polymer chain length. Nonetheless, this effectively demonstrates that the thiol−acrylate approach is a convenient and scalable procedure to enable installation of functional RAFTed polymers onto transparent glass slides. This method will enable the fabrication of more complex microarray surfaces, in particular for glycomics and cell-based assays where the interfacial properties of the surface of crucial for a successful experiment.

CONCLUSIONS

Here RAFTed, thermoresponsive polymers were investigated for their attachment to glass slides using thiol−ene chemistry as a versatile route to fabricate surfaces, for example, array applications. pOEGMA and pNIPAM were prepared by RAFT as two representative responsive polymers, bearing significantly different side chains with the pOEGMAs being brush-like in structure. The binding of the polymers onto acrylated glass and silicon substrates was investigated by drop shape analysis, and X-ray photoelectron spectroscopy confirmed covalent attachment and modification of the surface properties. The hydrophilic polymers were shown to effectively reduce the nonspecific absorption of a model protein compared to the native oxide surface. To quantitatively

DOI: 10.1021/acs.biomac.6b00662
Biomacromolecules 2016, 17, 2626−2633

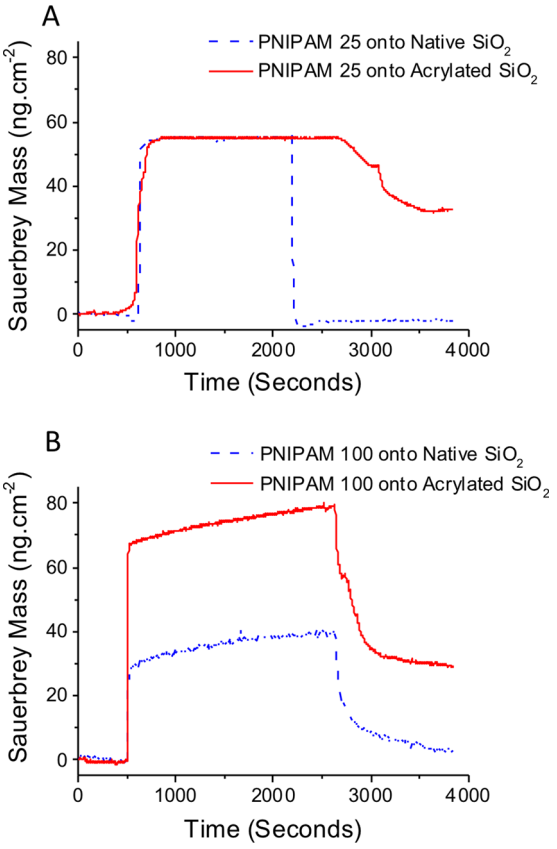

Figure 9. Sauerbrey mass values obtained from the adsorption of pNIPAM onto both acrylate silane functionalized and native silicon QCM sensors.

evaluate the efficiency of the grafting and compare to the widely used thiol−gold immobilization quartz crystal microbalance was employed. This revealed that the pNIPAMS resulted in much higher grafting densities than the pOEGMAs while crucial for array applications where the number of end-groups should be maximized. Compared to thiol−gold, lower densities were obtained suggesting the acrylate-coating was the limiting step. Overall this manuscript demonstrates a new and easy approach to generate polymer-coated glass slides that will find application in array applications, particularly for glycomics.

■ ASSOCIATED CONTENT

Supporting Information

The Supporting Information is available free of charge on the ACS Publications website at DOI: 10.1021/acs.biomac.6b00662.

Full details of the synthesis and characterization of RAFT agents; polymers alongside additional XPS and QCM-D spectra(PDF)

■ AUTHOR INFORMATION

Corresponding Author

*Email: m.i.gibson@warwick.ac.uk.

Notes

The authors declare no competing financial interest.

■ ACKNOWLEDGMENTS

Equipment used was supported by the Birmingham Science City (SC) Advanced Materials project with support from Advantage West Midlands and part funded by the European Regional Development Fund. M.I.G. was a Science City Research Fellow, supported HEFCE. C.I.B held a Ph.D. Scholarship from the BBSRC-funded Life Science Training Centre (BB/F017200/1). M.I.G. holds an ERC starter Grant (CRYOMAT 638661).

■ REFERENCES

(1) Ibanescu, S.-A.; Nowakowska, J.; Khanna, N.; Landmann, R.; Klok, H.-A. *Macromol. Biosci.* **2016**, *16* (5), 676−85.
(2) Zhai, L. *Chem. Soc. Rev.* **2013**, *42* (17), 7148−7160.
(3) Mendes, P. M. *Chem. Soc. Rev.* **2008**, *37* (11), 2512−2529.
(4) Zhernenkov, M.; Ashkar, R.; Feng, H.; Akintewe, O. O.; Gallant, N. D.; Toomey, R.; Ankner, J. F.; Pynn, R. *ACS Appl. Mater. Interfaces* **2015**, *7* (22), 11857−11862.
(5) Lutz, J. F.; Hoth, A. *Macromolecules* **2006**, *39* (2), 893−896.
(6) Alarcon, C.; Pennadam, S.; Alexander, C. *Chem. Soc. Rev.* **2005**, *34* (3), 276−285.
(7) Li, Z.; Kim, Y.-H.; Min, H. S.; Han, C.-K.; Huh, K. M. *Macromol. Res.* **2010**, *18* (6), 618−621.
(8) Alconcel, S. N. S.; Baas, A. S.; Maynard, H. D. *Polym. Chem.* **2011**, *2* (7), 1442−1448.
(9) Fan, X. W.; Lin, L. J.; Messersmith, P. B. *Biomacromolecules* **2006**, *7* (8), 2443−2448.
(10) Lowe, A. B. *Polym. Chem.* **2014**, *5* (17), 4820−4870.
(11) Yang, K.; Huang, X. Y.; Zhu, M.; Xie, L. Y.; Tanaka, T.; Jiang, P. K. *ACS Appl. Mater. Interfaces* **2014**, *6* (3), 1812−1822.
(12) Bhatt, S.; Pulpytel, J.; Arefi-Khonsari, F. *Surf. Innovations* **2015**, *3* (2), 63−83.
(13) Baghai, M.; Tamura, N.; Beyersdorf, F.; Henze, M.; Prucker, O.; Ruehe, J.; Goto, S.; Zieger, B.; Heilmann, C. *ASAIO J.* **2014**, *60* (5), 587−593.
(14) Chattopadhyay, S.; Heine, E.; Mourran, A.; Richtering, W.; Keul, H.; Moeller, M. *Polym. Chem.* **2016**, *7* (2), 364−369.
(15) Zhi, Z. L.; Laurent, N.; Powell, A. K.; Karamanska, R.; Fais, M.; Voglmeir, J.; Wright, A.; Blackburn, J. M.; Crocker, P. R.; Russell, D. A.; Flitsch, S.; Field, R. A.; Turnbull, J. E. *ChemBioChem* **2008**, *9* (10), 1568−1575.
(16) Sumerlin, B. S.; Lowe, A. B.; Stroud, P. A.; Zhang, P.; Urban, M. W.; McCormick, C. L. *Langmuir* **2003**, *19* (14), 5559−5562.
(17) Gibson, M. I.; Danial, M.; Klok, H.-A. *ACS Comb. Sci.* **2011**, *13* (3), 286−297.
(18) Richards, S.-J.; Fullam, E.; Besra, G. S.; Gibson, M. I. *J. Mater. Chem. B* **2014**, *2* (11), 1490−1498.
(19) Park, S.; Gildersleeve, J. C.; Blixt, O.; Shin, I. *Chem. Soc. Rev.* **2013**, *42* (10), 4310−4326.
(20) Banerjee, I.; Pangule, R. C.; Kane, R. S. *Adv. Mater.* **2011**, *23* (6), 690−718.
(21) Bebis, K.; Jones, M. W.; Haddleton, D. M.; Gibson, M. I. *Polym. Chem.* **2011**, *2* (4), 975−982.
(22) Phillips, D. J.; Gibson, M. I. *Chem. Commun.* **2012**, *48* (7), 1054−1056.
(23) Duwez, A. S.; Guillet, P.; Colard, C.; Gohy, J. F.; Fustin, C. A. *Macromolecules* **2006**, *39* (8), 2729−2731.
(24) Biggs, C. I.; Edmondson, S.; Gibson, M. I. *Biomater. Sci.* **2015**, *3* (1), 175−181.
(25) Wang, J.; Gibson, M. I.; Barbey, R.; Xiao, S. J.; Klok, H. A. *Macromol. Rapid Commun.* **2009**, *30* (9−10), 845−850.
(26) Quere, D. *Phys. A* **2002**, *313* (1−2), 32−46.
(27) Bittrich, E.; Burkert, S.; Mueller, M.; Eichhorn, K.-J.; Stamm, M.; Uhlmann, P. *Langmuir* **2012**, *28* (7), 3439−3448.
(28) Richards, S.-J.; Gibson, M. I. *ACS Macro Lett.* **2014**, *3* (10), 1004−1008.
(29) Hucknall, A.; Rangarajan, S.; Chilkoti, A. *Adv. Mater.* **2009**, *21* (23), 2441−2446.
(30) Ostuni, E.; Chapman, R. G.; Holmlin, R. E.; Takayama, S.; Whitesides, G. M. *Langmuir* **2001**, *17* (18), 5605−5620.
(31) Dixon, M. C. *J. Biomol. Technol.* **2008**, *19* (3), 151−8.
(32) Hook, F.; Kasemo, B.; Nylander, T.; Fant, C.; Sott, K.; Elwing, H. *Anal. Chem.* **2001**, *73* (24), 5796−5804.

DOI: 10.1021/acs.biomac.6b00662
Biomacromolecules 2016, 17, 2626−2633